mater.scichina.com link.springer.com

Published online 26 October 2023 | https://doi.org/10.1007/s40843-023-2595-8
Sci China Mater 2023, 66(11): 4437–4444

Indolo[3,2,1-*jk*]carbazole-derived planar electron transport materials realizing high efficiency in green phosphorescent organic light-emitting diodes

Sejeong Um[1], Unhyeok Jo[1] and Jun Yeob Lee[1,2,3*]

ABSTRACT **Two novel electron transporting materials (ETMs), 2-(4,6-diphenyl-1,3,5-triazin-2-yl)indolo[3,2,1-*jk*]-carbazole (DPTrz-ICz) and 5,11-bis(4,6-diphenyl-1,3,5-triazin-2-yl)-2-phenylindolo[3,2,1-*jk*]carbazole (2DPTrz-ICz), were developed based on the indolo[3,2,1-*jk*]carbazole (ICz) core, combined with 2,4-diphenyl-1,3,5-triazine (DPTrz). The introduced ICz core in ETM exhibited enhanced intermolecular charge transport properties owing to its planar and rigid geometry and high triplet energy, demonstrating the potential of designing ETM. Consequently, 2DPTrz-ICz, featuring high triplet energy of 2.84 eV, effectively prevented triplet exciton quenching and showed increased electron mobility owing to the activation of intermolecular hopping charge transfer facilitated by stacking architecture. The two materials were utilized as ETMs in green phosphorescent organic light-emitting diodes. 2DPTrz-ICz exhibited a superior external quantum efficiency of 21.5%, higher than that of the spirobifluorene-derived ETM.**

Keywords: electron transport layer, indolocarbazole, efficiency, OLED

INTRODUCTION

Developing organic light-emitting diodes (OLEDs) has opened an era of next-generation displays through unprecedented high-resolution, thinness, and flexibility and has supplemented the limitations of conventional liquid crystal displays, such as narrow viewing angle and slow response speed [1–5]. Although several OLED types have been developed, phosphorescent OLEDs (PHOLED) have been widely studied because they can realize an internal quantum efficiency of 100% *via* harvesting triplet excitons for light emission [6].

Many studies have been conducted on host molecules responsible for transporting charges in the emitting layer (EML) and dopant molecules that directly participate in light emission *via* recombining charges because both are critical to the efficiency and device lifetime of PHOLEDs [7–14]. However, the high efficiency of PHOLEDs cannot be realized without the assistance of hole transport material and electron transport material (ETM) injecting and transporting carriers into EML. Generally, electron mobility is inherently lower than hole mobility, which encourages the development of high-mobility ETM. There are three major requirements for ETM to increase the efficiency of PHOLED. (1) Good electron injection/hole blocking ability, which can be realized by adjusting the lowest unoccupied molecular orbital (LUMO) of the ETM to have an appropriate value to form a stepwise configuration between the LUMO of the EML and the work function (WF) of the cathode for efficient electron injection. Additionally, the highest occupied molecular orbital (HOMO) of the ETM should be much deeper than that of EML for charges to recombine only in the EML. (2) High electron mobility can be achieved by introducing an electron-deficient moiety with a heteroaromatic ring, such as triazine, pyridine, pyrimidine, and dibenzofuran, or *via* enlarging the π-conjugation of the core. (3) High triplet energy (E_T) can be obtained by introducing a high triplet energy moiety with a limited degree of conjugation. Because all excitons relax and emit light from the lowest triplet-excited state and have a relatively long lifetime (μs scale), the nonradiative loss should be minimized by suppressing triplet exciton quenching using high-triplet-energy ETMs. In addition to charge balance, requirements (1) and (2) can reduce the turn-on voltage (V_{on}) and driving voltage (V_d), respectively.

High-mobility ETMs derived from an anthracene core with a condensed π-conjugated structure have been previously studied [15–18]. Duan's group [15] recently reported an anthracene derivative ETM, DPPyA, taking advantage of high charge mobility *via* inter/intramolecular hydrogen bonds by adding pyridyl units to enable a facile electron hopping mechanism. However, owing to the incompatibility of high charge mobility and the high E_T of the large π-conjugated structure, DPPyA has a low E_T of 1.77 eV, which is insufficient to prevent triplet exciton leakage from the EML with green phosphor. ETMs using spiro structures that complement the low E_T of anthracene-based ETM have also been actively studied [19–24], because they can have a high E_T of ⩾2.3 eV using the sp^3 carbon connecting the two spiro moieties. 2,7-Bis(4,6-diphenyl-1,3,5-triazin-2-yl)-9,9′-spirobi[fluorene] (SBFTrz) with a high E_T of 2.53 eV was developed by adding an electron transporting triazine moiety to a spirobifluorene (SBF) core [23], which has an excellent ability for electron transport and efficient exciton blocking with the green phosphor in EML [25]. As a result, it showed lower V_{on}/V_d and higher efficiency than 2,8-bis(4,6-diphenyl-1,3,5-triazin-2-

[1] School of Chemical Engineering, Sungkyunkwan University 2066, Seobu-ro, Jangan-gu, Suwon, Gyeonggi, 16419, Republic of Korea
[2] SKKU Advanced Institute of Nano Technology, Sungkyunkwan University 2066, Seobu-ro, Jangan-gu, Suwon, Gyeonggi, 16419, Republic of Korea
[3] SKKU Institute of Energy Science and Technology, Sungkyunkwan University 2066, Seobu-ro, Jangan-gu, Suwon, Gyeonggi, 16419, Republic of Korea
* Corresponding author (email: leej17@skku.edu)

yl)dibenzo-[*b*,*d*]furan (DBFTrz), which has dibenzofuran as a core structure and is commonly used for ETL. However, ETMs for PHOLED must be further developed to upgrade the device performances of green PHOLED.

Herein, we designed two ETMs, 2-(4,6-diphenyl-1,3,5-triazin-2-yl)indolo[3,2,1-*jk*]carbazole (DPTrz-ICz) and 5,11-bis(4,6-diphenyl-1,3,5-triazin-2-yl)-2-phenylindolo[3,2,1-*jk*]carbazole (2DPTrz-ICz), *via* introducing indolo[3,2,1-*jk*]carbazole (ICz) core and 2,4-diphenyl-1,3,5-triazine (DPTrz) for high triplet energy and high electron mobility. The DPTrz-ICz and 2DPTrz-ICz showed high E_T values of 2.98 and 2.84 eV for triplet exciton blocking, respectively. Among the two ETMs, 2DPTrz-ICz particularly achieved a lower V_{on}/V_d (at 3000 cd m^{-2}) of 3.5 V/6.8 V and higher external quantum efficiency (EQE) of 21.5% than SBFTrz in device performances. This is owing to the quenching suppression effect because of the high triplet energy and the improved electron transport property obtained *via* inter/intramolecular interactions.

RESULTS AND DISCUSSION

Material design and synthesis

Conventionally, ICz has been mainly studied as a core structure of green or blue multiresonance emitter [26–28] because it can realize a narrow full width at half maximum and a small Stoke's shift owing to its rigid and planar structure and high singlet/triplet energy [29]. The planarity and rigidity of its structure can also strengthen the intermolecular interaction *via* molecular packing, facilitating the electron hopping mechanism between molecules and increasing electron mobility. Therefore, ICz is suitable as the core structure of the ETM, which requires high electron mobility and high triplet energy. In addition, the ICz has a higher triplet energy by 0.3 eV than SBF and is advantageous to prevent triplet exciton leakage from the emitter. In addition to high electron mobility and triplet energy, combining ICz with prominent DPTrz electron transport units can give ETMs a deep HOMO/LUMO value and low energy barrier for electron injection from the cathode. Furthermore, the nitrogen atoms of the triazine moiety form intramolecular hydrogen bonds with the hydrogen atoms of the ICz core, further strengthening the rigidity and planarity of the molecule for high electron mobility. Based on this concept, DPTrz-ICz and 2DPTrz-ICz with one DPTrz and two DPTrz units were developed.

To theoretically prove our design concept for the ETMs, density functional theory (DFT) calculation and time-dependent DFT (TD-DFT) calculation of the ETMs were performed using the Gaussian 16 program with B3LYP 6-31G* basis. As depicted in the side view of ETMs in Fig. 1a, the triazine and ICz moieties of both molecules are completely in the same plane, and only the 2DPTrz-ICz molecule has a phenyl group rotated by 41° at the C2 position of the ICz core. As expected, this suggests that the intramolecular hydrogen bond can be formed between the ICz and the DPTrz (red dash line in Fig. 1a). Since this geometry is advantageous for strengthening intermolecular stacking, it may contribute to expanding the electron transfer channel *via* increasing the π–π orbital overlap between molecules. The HOMO and LUMO distributions of the two ETMs are shown in Fig. 1b. The LUMO is distributed on the strongly electron-deficient triazine moiety, while the HOMO is dispersed on the weakly electron-rich ICz core. However, the HOMO and LUMO distributions are completely separated in the DPTrz-ICz, while LUMO is extended through the DPTrz and ICz units. This might positively impact electron mobility for electron hopping owing to extensive orbital overlap. Although the calculated triplet energy (2.84 eV) of 2DPTrz-ICz is slightly lower than that of DPTrz-ICz (2.98 eV), both molecules are expected to have high triplet energy to suppress triplet exciton quenching of green phosphors owing to the high triplet energy of the ICz moiety. In addition, the simulated HOMO–LUMO gap of 2DPTrz-ICz (3.69 eV) is smaller than that of DPTrz-ICz (3.92 eV), and the LUMO level of 2DPTrz-ICz is deeper than that of DPTrz-ICz owing to the extra DPTrz moiety in 2DPTrz-ICz.

The synthesis processes of DPTrz-ICz and 2DPTrz-ICz are schematically shown in Scheme 1. The two ETMs were synthesized as follows. The C2 position of 2-bromoindolo[3,2,1-*jk*]-carbazole (SM) was first substituted with a boronic ester group *via* borylation with bis(pinacolato)diboron (B_2pin_2), forming M1. DPTrz-ICz was then synthesized *via* Suzuki coupling between the boronic ester of M1 and the chlorine atom of the 2-

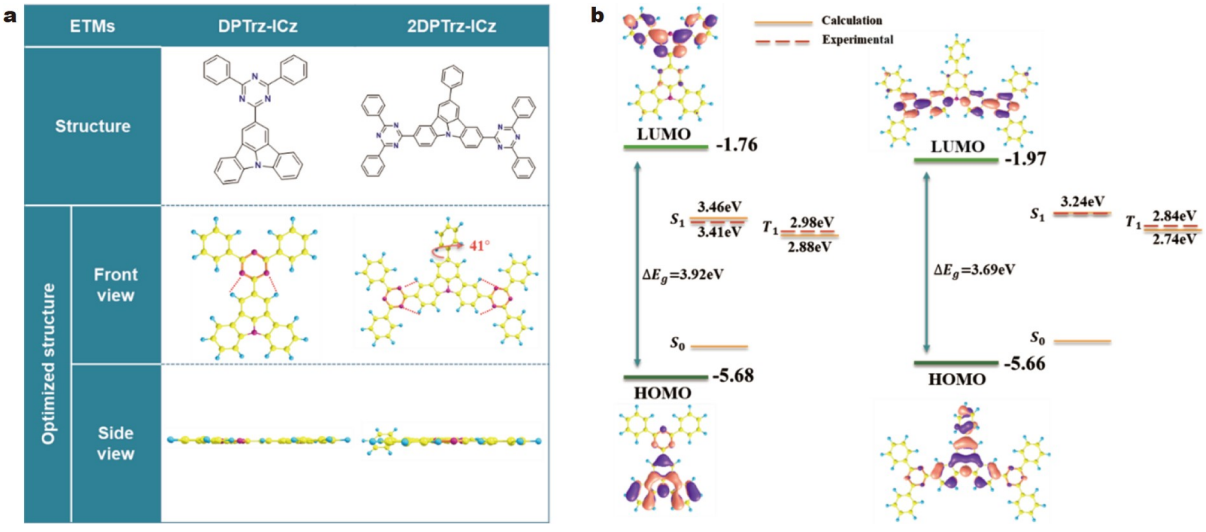

Figure 1 (a) Chemical structures and front/side view of the optimized structures of DPTrz-ICz and 2DPTrz-ICz using the Gaussian 16 program. (b) DFT/TD-DFT calculations of DPTrz-ICz (left) and 2DPTrz-ICz (right).

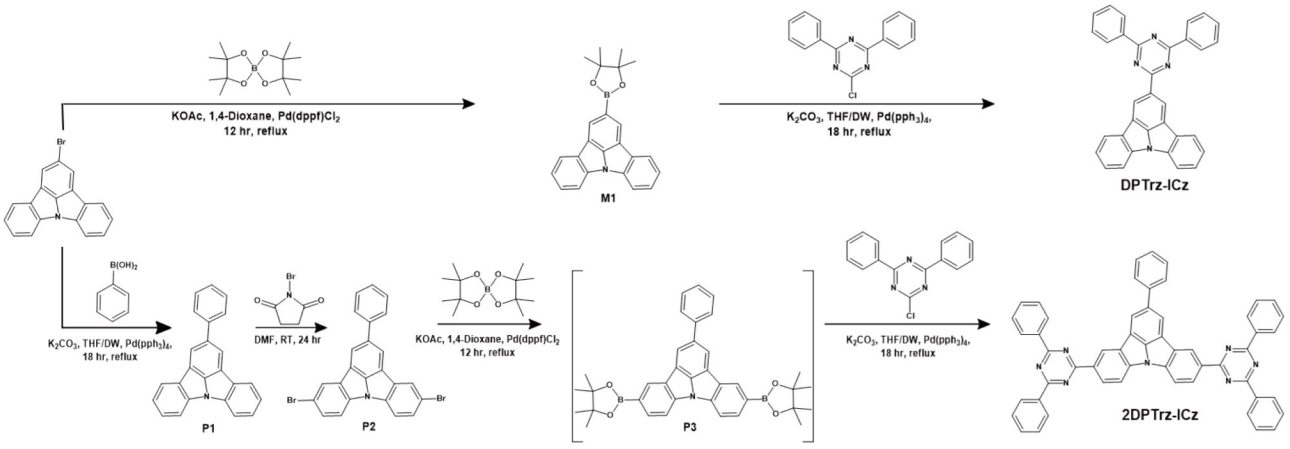

Scheme 1 Synthesis processes of DPTrz-ICz and 2DPTrz-ICz.

chloro-4,6-diphenyl-1,3,5-triazine (DPTrz–Cl). Moreover, P1 was obtained *via* Suzuki coupling between phenylboronic acid and SM, and P2 was synthesized following the procedure reported in our previous work [30]. Then, the bromine located at the 5 and 11 positions of the ICz core in P2 was substituted with boronic ester groups *via* borylation with B_2pin_2, forming P3. In this reaction step, mono- and di-substituted boronic esters were generated in the ratio of 2:8. The mixture was directly used in the subsequent reaction without separating the compounds. Finally, 2DPTrz-ICz was prepared *via* Suzuki coupling between P3 and DPTrz–Cl. Further details on the reaction conditions and reagents can be found in the Supplementary information.

Thermal analysis

Thermogravimetric analysis (TGA) and differential scanning calorimeter (DSC) measurements were conducted to determine the thermal stability of the two ETMs. Firstly, the decomposition temperature (T_d) at a weight loss of 5% from the initial weight of the organic matter was confirmed. The T_d of DPTrz-ICz and 2DPTrz-ICz were 402 and 550°C (Fig. 2c), respectively, and 2DPTrz-ICz showed excellent thermal stability, indicating that it can stably evaporate thermally with little decomposition at high temperatures. This results from the synergistic effect induced by the highly rigid ICz core and the hydrogen bonds from the triazine moiety. The DSC measurement was also performed for both molecules, but it was impossible to detect their glass transition temperature owing to planar and rigid geometry that limited the local motion of molecules.

Photophysical properties

To identify the photophysical properties, the ultraviolet-visible (UV-vis) absorption and photoluminescence (PL) spectra were measured at a concentration of 10^{-5} mol L^{-1} in tetrahydrofuran (THF) solvent, as depicted in Fig. 2a, b and summarized in Table 1. The UV-vis absorption spectra of both molecules showed π–π^* transitions at wavelengths below 300 nm and n–π^* transitions at 300–400 nm. The 2DPTrz-ICz tended to absorb light at longer wavelengths owing to its extended conjugation within the backbone structure. The HOMO–LUMO gap estimated from the absorption onset was smaller in 2DPTrz-ICz (3.11 eV) than that in DPTrz-ICz (3.23 eV), consistent with the theoretical calculation. PL spectra were also analyzed to investigate the fluorescence and phosphorescence properties. DPTrz-ICz and 2DPTrz-ICz exhibited similar peak wavelengths of 398 and 401 nm in THF at 273 K. Low temperature (77 K) PL measurements of DPTrz-ICz and 2DPTrz-ICz offered high triplet energy of 2.98 and 2.84 eV, respectively, owing to the high triplet energy of the ICz, which was higher than that of previously reported SBFTrz. This proves both compounds can be excellent ETMs to prevent triplet exciton quenching from green phosphorescent dopant.

The triplet exciton blocking effect of the ETMs was analyzed using transient PL (TRPL) measurement. The TRPL measurement was conducted using 2DPTrz-ICz film doped with 5% tris-(2-phenylpyridine)iridium ($Ir(ppy)_3$), SBFTrz doped with $Ir(ppy)_3$, and 2-phenyl-4,6-bis(12-phenylindolo[2,3-*a*]carbazole-11-yl)-1,3,5-triazine (PBICT):4-(3-(triphenylene-2-yl)phenyl)-dibenzo-[*b*,*d*]thiophene (DBTTP1) (75:25) film doped with $Ir(ppy)_3$ (Fig. 2d and Table S1). The PBICT:DBTTP1 film was used as a control sample because it was used as a host in the fabrication of the devices. The fluorescence decay curve of the 2DPTrz-ICz film was similar to that of the PBICT:DPTTP1 film, suggesting that the triplet excitons of $Ir(ppy)_3$ were not quenched by the 2DPTrz-ICz of ETM owing to its high triplet energy. However, the SBFTrz film displayed a completely distinct decay pattern from the other two curves, suggesting a triplet exciton quenching of the emitter by SBFTrz. Furthermore, PL quantum yield (PLQY) was measured to determine the luminous efficiency of the three $Ir(ppy)_3$-doped films. Consistent with the TRPL trend, the 2DPTrz-ICz film showed a high PLQY of 92.3% compared with that of the control sample (96.0%), while the SBFTrz film demonstrated a considerably low efficiency of 24.8% owing to its triplet exciton quenching. Therefore, the TRPL and PLQY measurements infer that 2DPTrz-ICz is a more suitable ETM for enhancing EQE *via* effectively confining the triplet exciton within the EML in green PHOLED.

Device characteristics

To investigate the electron transport characteristics of each molecule when incorporated into a device, the electron-only device was fabricated with the following configuration for the developed ETMs: indium tin oxide (ITO, 50 nm)/dphenyl[4-(triphenylsilyl)phenyl]phosphine oxide (TSPO1, 10 nm)/ETMs (60 nm)/LiF (1.5 nm)/Al (200 nm). TSPO1 was used as a hole-blocking layer. The ETMs were DPTrz-ICz, 2DPTrz-ICz, and

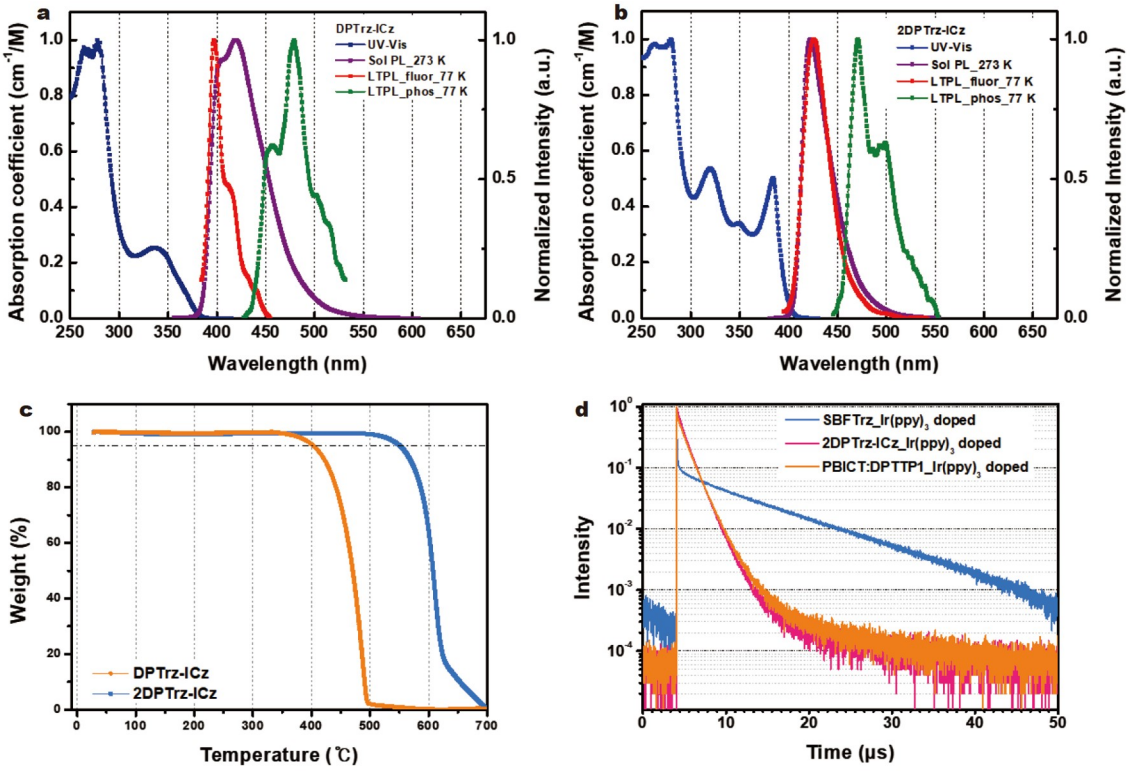

Figure 2 UV-vis absorption spectra, fluorescence spectra (273 K/77 K), and phosphorescence spectra at 77 K of 10^{-5} mol L^{-1} in THF solutions of (a) DPTrz-ICz and (b) 2DPTrz-ICz. (c) TGA curves of DPTrz-ICz and 2DPTrz-ICz. (d) TRPL of 5 wt% $Ir(ppy)_3$-doped 2DPTrz-ICz, SBFTrz, and PBICT:DBTTP1 (75:25).

Table 1 Photophysical and electrochemical properties and thermal stability of 2DPTrz-ICz and DPTrz-ICz

	λ_{ab}[a] (nm)	$\lambda_{em,max}$[b] (nm)	E_S[c/d] (eV)	E_T[e/f] (eV)	E_g (eV)	HOMO/LUMO[g] (eV)	T_d[h] (°C)
DPTrz-ICz	381	398	3.41/3.31	2.98/2.68	3.23	−5.71/−2.48	402
2DPTrz-ICz	398	401	3.24/3.06	2.84/2.73	3.11	−6.13/−3.02	550

a) Onset wavelength of UV-vis absorption spectra in THF solution (10^{-5} mol L^{-1}, 273 K). b) The peak wavelength of the PL spectra in THF solution (10^{-5} mol L^{-1}, 273 K). c) The onset and d) peak wavelength of low-temperature fluorescence in frozen THF (10^{-5} mol L^{-1}, 77 K). e) The onset and f) peak wavelength of low-temperature phosphorescence in frozen THF (10^{-5} mol L^{-1}, 77 K). g) Ionization energy (HOMO) derived from UV photoelectron spectroscopy, $E_{LUMO} = E_{HOMO} + E_g$. h) Decomposition temperature at which the weight loss of 5% from the initial weight occurs.

SBFTrz. Fig. 3a shows that the electron current density of 2DPTrz-ICz is considerably higher than that of DPTrz-ICz and even superior to that of SBFTrz. This can be attributed to the planar ICz core compared with the sp^3 carbon-based SBF core. The almost-planar molecular backbone structure and widespread LUMO promoted electron hopping between 2DPTrz-ICz molecules. However, the electron current density of DPTrz-ICz was considerably lower than that of the other two molecules, possibly owing to localized LUMO distribution. The electron mobility values measured using impedance spectroscopy at 1.25×10^6 V cm^{-1} for DPTrz-ICz, 2DPTrz-ICz, and SBFTrz were 2.35×10^{-8}, 9.00×10^{-7}, and 6.13×10^{-7} cm^{-2} V^{-1} s^{-1}, respectively (Fig. 3b). The high electron mobility of 2DPTrz-ICz, which is ~1.5 times higher than that of SBFTrz, is derived from its flat and robust molecular structure. The planar geometry of 2DPTrz-ICz induces a densely packed architecture in the film, enhancing the strong overlap of p-orbitals between adjacent molecules. Consequently, the electrons in the p-orbital can easily move to neighbor molecules *via* phonon and electronic vibronic coupling caused by the vibration of the organic molecules, activating hopping transport [31].

The molecular packing of 2DPTrz-ICz was indirectly analyzed by monitoring the peak wavelength changes in solution and solid films. The PL spectra of 2DPTrz-ICz and SBFTrz were measured by changing the solvent composition of the THF/water mixed solvent. As shown in Fig. S1, the change in the PL peak wavelength owing to intermolecular interaction was observed by inducing the precipitation of the molecules in a water-rich solvent. After aggregation, 2DPTrz-ICz showed a bathochromic shift of 43 nm, while SBFTrz showed a maximum shift of 6 nm. This result presumes that the intermolecular interaction of 2DPTrz-ICz is stronger than that of SBFTrz, facilitating electron hopping. In addition, an anionic reorganization was calculated because it is one of the critical factors affecting the electron mobility of organic materials [32–35]. The calculation results are shown in Fig. 3c. 2DPTrz-ICz had a lower reorganization energy of 1.253 eV compared with 1.475 eV for SBFTrz, indicating that 2DPTrz-ICz can enhance the electron

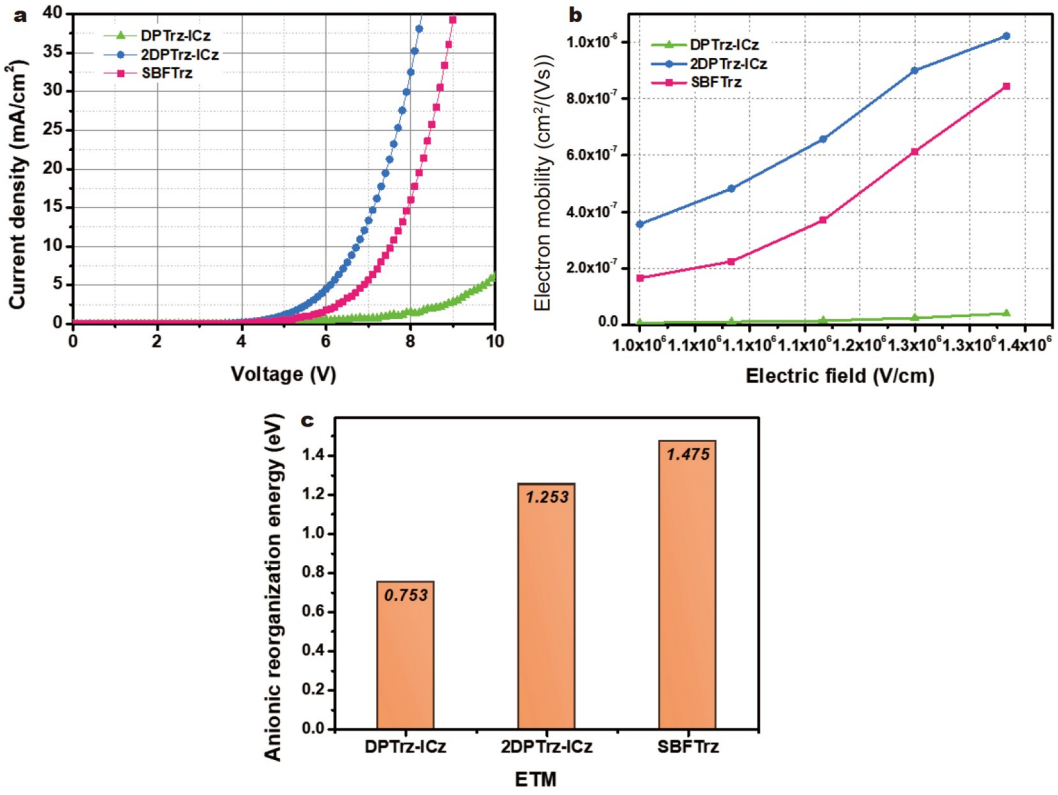

Figure 3 (a) Current density-voltage curves of 2DPTrz-ICz, DPTrz-ICz, and SBFTrz electron-only devices. (b) Electric field *versus* electron mobility curves of DPTr-ICz, 2DPTrz-ICz, and SBFTrz using impedance measurement. (c) Comparison of the anionic reorganization energies of 2DPTrz-ICz, DPTrz-ICz, and SBFTrz.

transport *via* the hopping process. Therefore, the low reorganization energy and extensive orbital overlap *via* the planar molecular geometry are responsible for the high electron mobility of 2DPTrz-ICz. In the case of DPTrz-ICz, despite the lowest reorganization energy of 0.753 eV, its electron mobility was smaller than that of 2DPTrz-ICz. This can be attributed to the influence of poor orbital overlap by the localized distribution of the LUMO solely on the triazine moiety as supported by DFT calculations. Additionally, the lack of an electron-deficient group sufficient to offset the hole transport property of ICz appears to be a contributing factor to the reduced electron mobility. To demonstrate this, we fabricated hole-only devices using the following structure to investigate the hole transporting characteristics of three ETMs: ITO (50 nm)/poly(3,4-ethylenedioxythiophene):poly(styrene sulfonate) (PEDOT:PSS, 40 nm)/*N*-([1,1′-biphenyl]-4-yl)-9,9-dimethyl-*N*-(4-(9-phenyl-9*H*-carbazol-3-yl)phenyl)-9*H*-fluoren-2-amine (BCFN, 10 nm)/ETMs (50 nm)/BCFN (20 nm)/Al (200 nm). As shown in Fig. S2, the current density with increasing voltage reveals prominent characteristics of hole transport in DPTrz-ICz. These bipolar properties of DPTrz-ICz compromise the electron mobility compared with other ETMs. On the other hand, for 2DPTrz-ICz, the hole transport characteristics of ICz are almost offset, confirming the unipolar behavior for electrons.

The green PHOLEDs with the following layer configuration (Fig. 4a) were fabricated to evaluate the performance of novel ETMs on a device level: ITO (50 nm)/*N*,*N*′-diphenyl-*N*,*N*′-bis-[4-(phenyl-*m*-tolyl-amino)-phenyl]-biphenyl-4,4′-diamine (DNTPD, 60 nm)/BCFN (20 nm)/9,9-dimethyl-10-(9-phenyl-9*H*-carbazol-2-yl)-9,10-dihydro-acridine (PCzAc, 10 nm)/DBTTP1:PBICT:Ir(ppy)$_3$ (30 nm, dope concentration = 25:75:5)/ETM (35 nm)/LiF (1.5 nm)/Al (200 nm). ITO was utilized as the anode, and LiF/Al was used as the cathode. DNTPD was used as a hole injection layer. BCFN and PCzAc acted as the hole transport and electron blocking layers, respectively. Then, DBTTP1:PBICT (25:75) was used as the cohost in EML, and DPTrz-ICz, 2DPTrz-ICz, and SBFTrz were employed as the ETL for each device.

As shown in Fig. 4b–e and Table 2, 2DPTrz-ICz showed a low V_{on} of 3.5 V and low V_d of 6.8 V at a brightness of 3000 cd m^{-2} owing to its previously demonstrated high electron mobility and the designed step-like configuration of LUMO level for the charge to overcome the energy barrier between the WF of the cathode and the LUMO of EML. Notably, it exhibited an enhanced EQE$_{max}$ of 21.5%, higher than that of the previously reported SBFTrz, owing to the higher triplet energy of 0.3 eV in 2DPTrz-ICz than that of Ir(ppy)$_3$ [25], as compared in the diagram in Fig. 4a. This suggests that 2DPTrz-ICz can effectively prevent triplet exciton leakage from EML, increasing its recombination efficiency. Furthermore, the power efficiency was also improved using 2DPTrz-ICz ETM. In contrast, DPTrz-ICz showed considerably high V_{on} (5.1 V) and V_d (10.8 V), which can be attributed to the considerably shallow LUMO of the ETM, resulting in a high electron injection barrier from the electrode. And also, despite the small reorganization energy and high triplet energy (2.98 eV), it exhibited underperformed EQE and η_{PE} due to the poor charge balance caused by low electron mobility and shallow HOMO/LUMO levels. Meanwhile, the electroluminescence (EL) wavelength analysis revealed that DPTrz-ICz and 2DPTrz-ICz exhibited a low-intense secondary

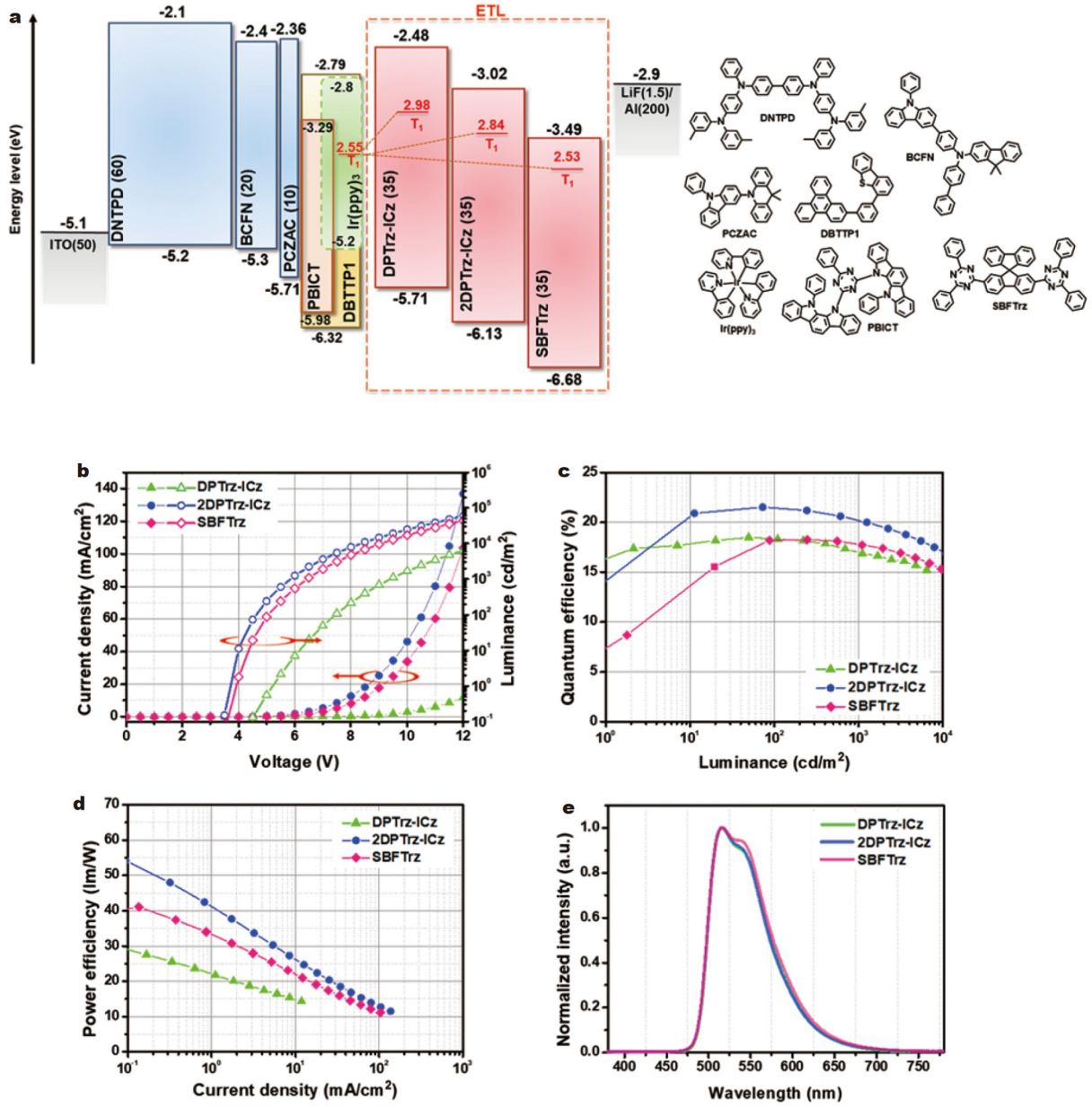

Figure 4 (a) Device configuration of green PHOLED. (b) Current density (*J*)-voltage (*V*)-luminance (*L*) curves; (c) EQE curves based on luminance; (d) the curves of current density *versus* power efficiency; (e) the EL wavelength curves of the devices using different ETMs.

peak at 540 nm compared with SBFTrz, indicating the advantages of our ETMs in achieving high-color purity green emission. Furthermore, the device lifetime was measured at 3000 cd m^{-2}, and 2DPTrz-ICz showed similar degradation to SBFTrz, demonstrating good stability of 2DPTrz-ICz (Fig. S3). This potential of 2DPTrz-ICz as an ETM in green PHOLED is attributed not only to the inherent property of ICz with a high triplet energy than SBF but also to the enhanced intermolecular charge transfer *via* the fused core and the vigorous activation of intramolecular charge transfer *via* the flat and robust molecular geometry. Therefore, this study confirms the potential of ICz as an ETM beyond the conventional application as an emitter, providing a new paradigm for designing future ETMs.

In addition, in order to confirm the versatility of ETMs in yellow PhOLED (Fig. S4) as well as green PhOLED, yellow PhOLEDs were fabricated using the following device configuration: ITO (50 nm)/DNTPD (60 nm)/BCFN (20 nm)/PCzAc (10 nm)/CzTrz:PO-01 (30 nm, 5 wt% doped)/ETM (35 nm)/LiF (1.5 nm)/Al (200 nm). As a yellow phosphorescent dopant, iridium(III) bis(4-phenylthieno[3,2,-*c*]pyridinato-*N*,*C*2′)acetylacetonate (PO-01), which showed high PLQY and intersystem crossing rate (ISC rate) [36], was employed and 9-(3′-(4,6-diphenyl-1,3,5-triazin-2-yl)-[1,1′-biphenyl]-3-yl)-9*H*-carbazole (CzTrz) was applied as the host material. The yellow PhOLED employing 2DPTrz-ICz ETM achieved a maximum EQE of 24.1%, demonstrating the universality of 2DPTrz-ICz as an ETL in yellow PhOLED (Table S2).

CONCLUSION

Herein, two ETMs, DPTrz-ICz and 2DPTrz-ICz, were developed

Table 2 EL performance data for each device using DPTrz-ICz, 2DPTrz-ICz, and SBFTrz

	V_{on}[a] (V)	V_d[b] (V)	EQE (%)[c] (3000 cd m^{-2})/Max	η_{PE} (lm W^{-1})[d] (3000 cd m^{-2})/Max	η_{CE} (cd A^{-1})[e] (3000 cd m^{-2})/Max	Color coord. (x,y)
DPTrz-ICz	5.1	10.8	16.2/18.5	16.9/35.6	57.9/66.4	(0.32,0.62)
2DPTrz-ICz	3.5	6.8	19.0/21.5	31.8/59.1	68.5/77.6	(0.32,0.62)
SBFTrz	3.8	7.4	17.0/18.2	25.7/41.0	60.8/65.5	(0.32,0.62)

a) Turn-on voltage at 1 cd m^{-2}. b) Driving voltage at 3000 cd m^{-2}. c) EQE at 3000 cd m^{-2}, maximum. d) Power efficiency at 3000 cd m^{-2}, maximum. e) Current efficiency at 3000 cd m^{-2}, maximum, of each device.

using ICz as a core. The ICz core, which possesses both planarity and robustness, was coupled with triazine to induce molecular stacking, thereby contributing to enhanced intermolecular charge transfer and electron mobility *via* reinforcing p-orbital overlap. Moreover, the high triplet energy of ICz effectively prevented triplet exciton leakage from EML. Furthermore, incorporating two DPTrz moieties into 2DPTrz-ICz effectively reduced the energy barrier to electron injection between the cathode and the emissive layer. As a result, compared with the previously reported SBFTrz core, the developed ETM showed excellent device performance, including a high EQE of 21.5% and a low V_{on} of 3.5 V, and it had a positive impact on achieving high-purity green emission.

Received 9 May 2023; accepted 25 August 2023; published online 26 October 2023

1 Hong G, Gan X, Leonhardt C, *et al.* A brief history of OLEDs—Emitter development and industry milestones. Adv Mater, 2021, 33: 2005630
2 Tang CW, VanSlyke SA. Organic electroluminescent diodes. Appl Phys Lett, 1987, 51: 913–915
3 Xu RP, Li YQ, Tang JX. Recent advances in flexible organic light-emitting diodes. J Mater Chem C, 2016, 4: 9116–9142
4 Chen HW, Lee JH, Lin BY, *et al.* Liquid crystal display and organic light-emitting diode display: Present status and future perspectives. Light Sci Appl, 2018, 7: 17168
5 Tao J, Wang R, Yu H, *et al.* Highly transparent, highly thermally stable nanocellulose/polymer hybrid substrates for flexible OLED devices. ACS Appl Mater Interfaces, 2020, 12: 9701–9709
6 Baldo MA, O'Brien DF, You Y, *et al.* Highly efficient phosphorescent emission from organic electroluminescent devices. Nature, 1998, 395: 151–154
7 Ihn SG, Lee N, Jeon SO, *et al.* An alternative host material for long-lifespan blue organic light-emitting diodes using thermally activated delayed fluorescence. Adv Sci, 2017, 4: 1600502
8 Sasabe H, Toyota N, Nakanishi H, *et al.* 3,3′-Bicarbazole-based host materials for high-efficiency blue phosphorescent OLEDs with extremely low driving voltage. Adv Mater, 2012, 24: 3212–3217
9 Song X, Zhang D, Lu Y, *et al.* Understanding and manipulating the interplay of wide-energy-gap host and TADF sensitizer in high-performance fluorescence OLEDs. Adv Mater, 2019, 31: 1901923
10 Chaskar A, Chen HF, Wong KT. Bipolar host materials: A chemical approach for highly efficient electrophosphorescent devices. Adv Mater, 2011, 23: 3876–3895
11 Kim YS, Lim J, Lee JY, *et al.* Rational management of charge transfer character of benzothienopyrimidine-based n-type host for blue phosphorescent organic light-emitting diodes. Adv Opt Mater, 2022, 10: 2101435
12 Kothavale SS, Lee JY. Three- and four-coordinate, boron-based, thermally activated delayed fluorescent emitters. Adv Opt Mater, 2020, 8: 2000922
13 Im Y, Byun SY, Kim JH, *et al.* Recent progress in high-efficiency blue-light-emitting materials for organic light-emitting diodes. Adv Funct Mater, 2017, 27: 1603007
14 Wong MY, Zysman-Colman E. Purely organic thermally activated delayed fluorescence materials for organic light-emitting diodes. Adv Mater, 2017, 29: 1605444
15 Zhang D, Qiao J, Zhang D, *et al.* Ultrahigh-efficiency green PHOLEDs with a voltage under 3 V and a power efficiency of nearly 110 lm W^{-1} at luminance of 10 000 cd m^{-2}. Adv Mater, 2017, 29: 1702847
16 Ye S, Wang Y, Guo R, *et al.* Asymmetric anthracene derivatives as multifunctional electronic materials for constructing simplified and efficient non-doped homogeneous deep blue fluorescent OLEDs. Chem Eng J, 2020, 393: 124694
17 Zhang D, Wei P, Zhang D, *et al.* Sterically shielded electron transporting material with nearly 100% internal quantum efficiency and long lifetime for thermally activated delayed fluorescent and phosphorescent OLEDs. ACS Appl Mater Interfaces, 2017, 9: 19040–19047
18 Zhang D, Song X, Li H, *et al.* High-performance fluorescent organic light-emitting diodes utilizing an asymmetric anthracene derivative as an electron-transporting material. Adv Mater, 2018, 30: 1707590
19 Guo X, Bian M, Lv F, *et al.* Increasing electron transporting properties and horizontal molecular orientation *via* meta-position of nitrogen for "$(A)_n$–D–$(A)_n$" structured terpyridine electron-transporting material. J Mater Chem C, 2019, 7: 11581–11587
20 Guo X, Tang Z, Yu W, *et al.* A high thermal stability terpyridine derivative as the electron transporter for long-lived green phosphorescent OLED. Org Electron, 2021, 89: 106048
21 Bian M, Zhang D, Wang Y, *et al.* Long-lived and highly efficient TADF-PhOLED with "$(A)_n$–D–$(A)_n$" structured terpyridine electron-transporting material. Adv Funct Mater, 2018, 28: 1800429
22 Kang JA, Chan Kim S, Lee JY. Isomer engineering of universal electron transport materials for suppressed exciton quenching in organic light-emitting diodes. Dyes Pigments, 2022, 203: 110319
23 Kang JA, Lim J, Lee JY. Spirobifluorene modified electron transport materials for high efficiency in phosphorescent organic light-emitting diodes. Mater Chem Front, 2022, 6: 757–764
24 Duan K, Zhu Y, Liu Z, *et al.* A wide-bandgap, high-mobility electron-transporting material containing a 9,9′-spirobithioxanthene skeleton. Chem Eng J, 2022, 429: 132215
25 Su SJ, Tanaka D, Li YJ, *et al.* Novel four-pyridylbenzene-armed biphenyls as electron-transport materials for phosphorescent OLEDs. Org Lett, 2008, 10: 941–944
26 Luo XF, Song SQ, Ni HX, *et al.* Multiple-resonance-induced thermally activated delayed fluorescence materials based on indolo[3,2,1-*jk*]carbazole with an efficient narrowband pure-green electroluminescence. Angew Chem Int Ed, 2022, 61: e202209984
27 Wei J, Zhang C, Zhang D, *et al.* Indolo[3,2,1-*jk*]carbazole embedded multiple-resonance fluorophors for narrowband deep-blue electroluminescence with EQE ≈ 34.7 % and CIE$_y$ ≈ 0.085. Angew Chem Int Ed, 2021, 60: 12269–12273
28 Lee HL, Jeon SO, Kim I, *et al.* Multiple-resonance extension and spin-vibronic-coupling-based narrowband blue organic fluorescence emitters with over 30% quantum efficiency. Adv Mater, 2022, 34: 2202464
29 Bader D, Fröhlich J, Kautny P. Thienopyrrolo[3,2,1-*jk*]carbazoles: Building blocks for functional organic materials. J Org Chem, 2019, 85: 3865–3871
30 Patil VV, Lee KH, Lee JY. Universal blue emitters for high efficiency thermally activated delayed fluorescence and fluorescent organic light-emitting diodes. Dyes Pigments, 2020, 174: 108070

31 Coropceanu V, Cornil J, da Silva Filho DA, *et al.* Charge transport in organic semiconductors. Chem Rev, 2007, 107: 926–952
32 Brückner C, Engels B. A theoretical description of charge reorganization energies in molecular organic p-type semiconductors. J Comput Chem, 2016, 37: 1335–1344
33 Yang B, Kim SK, Xu H, *et al.* The origin of the improved efficiency and stability of triphenylamine-substituted anthracene derivatives for OLEDs: A theoretical investigation. ChemPhysChem, 2008, 9: 2601–2609
34 Lin BC, Cheng CP, Lao ZPM. Reorganization energies in the transports of holes and electrons in organic amines in organic electroluminescence studied by density functional theory. J Phys Chem A, 2003, 107: 5241–5251
35 Surukonti N, Kotamarthi B. Mono substituted pyrenes as multifunctional materials for OLED: Analysis of the substituent effects on the charge transport properties using DFT methods. Comput Theor Chem, 2018, 1138: 48–56
36 Wang H, Zhao H, Zang C, *et al.* Stable and efficient phosphorescent organic light-emitting device utilizing a δ-carboline-containing host displaying thermally activated delayed fluorescence. J Mater Chem C, 2020, 8: 3800–3806

Acknowledgements This work was supported by Ministry of Trade, Industry and Energy (MOTIE) (20012622 and P0017363).

Author contributions Um S designed and synthesized the materials; Jo U fabricated and evaluated the devices; Lee JY wrote the manuscript and supervised the research. All authors reviewed and approved the final manuscript.

Conflict of interest The authors declare that they have no conflict of interest.

Supplementary information Experimental details and supporting data are available in the online version of the paper.

Sejeong Um received her Bachelor's degree in chemical engineering/polymer engineering from Sungkyunkwan University (2018–2022). After that, she earned her Master's degree in chemical engineering from Sungkyunkwan University (2022–2023) by conducting the research on the design and synthesis of organic electronic materials for electron transport in organic light-emitting diodes.

Unhyeok Jo received his BSc degree from the Department of Semiconductor and Physical electronics, Sangji University, Republic of Korea. He is now a Master candidate at the Department of Chemical Engineering, Sungkyunkwan University, Republic of Korea. His main research areas are the development of exciton dynamics and emission mechanism for organic light-emitting diodes.

Jun Yeob Lee received his PhD degree from Seoul National University, Republic of Korea in 1998. After postdoc at Rensselaer Polytechnic Institute (1998–1999), he joined Samsung SDI and developed active matrix organic light-emitting diodes for six years. After that, he worked as a professor at the Department of Polymer Science and Engineering, Dankook University. He has been a professor at the School of Chemical Engineering, Sungkyunkwan University since 2015. His main research areas are the synthesis of organic electronic materials and development of novel device structures for organic electronic devices.